2019

A 3D-Printed Omni-Purpose Soft Gripper

Charbel Tawk
University of Wollongong, charbel@uow.edu.au

Andrew Gillett
University of Wollongong

Marc in het Panhuis
University of Wollongong, panhuis@uow.edu.au

Geoffrey M. Spinks
University of Wollongong, gspinks@uow.edu.au

Gursel Alici
University of Wollongong, gursel@uow.edu.au

A 3D-Printed Omni-Purpose Soft Gripper

Abstract

Numerous soft grippers have been developed based on smart materials, pneumatic soft actuators, and underactuated compliant structures. In this article, we present a three-dimensional (3-D) printed omni-purpose soft gripper (OPSOG) that can grasp a wide variety of objects with different weights, sizes, shapes, textures, and stiffnesses. The soft gripper has a unique design that incorporates soft fingers and a suction cup that operate either separately or simultaneously to grasp specific objects. A bundle of 3-D-printable linear soft vacuum actuators (LSOVA) that generate a linear stroke upon activation is employed to drive the tendon-driven soft fingers. The support, fingers, suction cup, and actuation unit of the gripper were printed using a low-cost and open-source fused deposition modeling 3-D printer. A single LSOVA has a blocked force of 30.35 N, a rise time of 94 ms, a bandwidth of 2.81 Hz, and a lifetime of 26 120 cycles. The blocked force and stroke of the actuators are accurately predicted using finite element and analytical models. The OPSOG can grasp at least 20 different objects. The gripper has a maximum payload-to-weight ratio of 7.06, a grip force of 31.31 N, and a tip blocked force of 3.72 N.

Disciplines

Engineering | Science and Technology Studies

Publication Details

Tawk, C., Gillett, A., in het Panhuis, M., Spinks, G. M. & Alici, G. (2019). A 3D-Printed Omni-Purpose Soft Gripper. IEEE Transactions on Robotics, 35 (5), 1268-1275.

A 3D Printed Omni-Purpose Soft Gripper

Charbel Tawk, Andrew Gillett, Marc in het Panhuis, Geoffrey M. Spinks, and Gursel Alici*

***Abstract*—Numerous soft grippers have been developed based on smart materials, pneumatic soft actuators and underactuated compliant structures. In this work, we present a 3D printed omni-purpose soft gripper (OPSOG) that can grasp a wide variety of objects with different weights, sizes, shapes, textures and stiffnesses. The soft gripper has a unique design that incorporates soft fingers and a suction cup that operate either separately or simultaneously to grasp specific objects. A bundle of 3D printable linear soft vacuum actuators (LSOVA) that generate a linear stroke upon activation is employed to drive the tendon-driven soft fingers. The support, fingers, suction cup and actuation unit of the gripper were printed using a low-cost and open-source fused deposition modeling 3D printer. A single LSOVA has a blocked force of 30.35N, a rise time of 94ms, a bandwidth of 2.81Hz and a lifetime of 26120 cycles. The blocked force and stroke of the actuators are accurately predicted using finite element and analytical models. The OPSOG can grasp at least 20 different objects. The gripper has a maximum payload-to-weight ratio of 7.06, a grip force of 31.31N and a tip blocked force of 3.72N.**

***Index Terms*—soft grasping, soft actuator, soft gripper, soft material robot.**

I. Introduction

THE soft robotics field has expanded rapidly in recent years during which many potential soft robots have emerged [1]. Unlike conventional robotic systems which are made entirely of rigid materials, soft robotic systems are primarily made of highly compliant and deformable materials. Conventional robots are very popular and useful in many industries and factories since they provide large forces, high precision, high accuracy and large speeds on assembly and automation lines [2]. However, these robotic systems have a very limited presence in close proximity with humans due to safety issues [3]. The compliance of soft robots, which is an intrinsic property of soft and deformable structures, allows them to collaborate and operate safely alongside humans as well as to conform to objects they interact with in unstructured environments.

Soft robots are inspired by soft biological structures such as octopus arms, squid tentacles, elephant trunk and worms [4]. One of the most fascinating biological structures that have inspired roboticists is the human hand as it is one of the most dexterous systems in nature [5]. The development of anthropomorphic end-effectors for robotic manipulation is largely based on human hand models [5]. Many grippers that are based on conventional robotic systems have been developed for robotic manipulation [6]. Recently, many soft grippers have been proposed where the fingers of the grippers are made of soft, smart and compliant materials and structures [7]. Soft grippers can grasp delicate objects without damaging them since the contact forces are reduced.

There are two main classes of soft grippers. In the first class, the fingers of the grippers are made of deformable materials and driven by some external soft or rigid actuators. In the second class, the soft fingers of the grippers are the actuators themselves. Electric motors are the most widely used external actuators in the first class of soft grippers. Tendon-driven soft grippers coupled with electric motors have been developed based on multiple techniques including fused deposition modeling (FDM) 3D printing [8,9], silicone molding [10] and assembled hybrid structures made of soft and rigid materials [11-13]. Other soft grippers and robotic hands use electric motors to drive compliant and adaptive bioinspired soft structures [14-15]. Smart materials, smart structures and soft pneumatic actuators are widely used in the second class of soft grippers. Smart and soft materials and structures such as shape memory alloys [16-20], shape memory polymers [21-23], dielectric elastomers [24-26], hydrogels [27-30], ionic polymer-metal composites [31,32] and humidity-responsive materials [33,34] have been used to develop grippers for soft robotic applications. Although the smart materials considered have several soft robotic applications, they are not yet capable of delivering acceptable performance in industrial gripping applications due to low actuation speed in shape memory alloys, shape memory polymers and hydrogels, low actuation forces in IPMCs and humidity-responsive materials and fatigue in dielectric elastomers.

Soft pneumatic actuators are one of the most adapted and studied actuators for developing soft grippers. Positive-pressure pneumatic network (PneuNet) actuators involving distinct designs have been used to develop soft grippers to achieve different modes of deformation [35], enhance gripping capabilities [36-38] and introduce new soft material properties such as self-healing [39]. Bellow-like pneumatic actuators were considered for commercial gripping and manipulation applications [40]. Fiber-reinforced soft actuators were used to develop soft hands [41,42] and adaptive soft grippers [43,44]. Soft pneumatic actuators combined with rigid structures were also used to develop soft grippers [45]. Furthermore, negative-pressure soft actuators were used to develop soft grippers such as granular jamming based universal soft grippers [46], bioinspired grippers based on passive and active soft suction cups [47] and low-cost soft grippers based on origami structures [48]. Many soft positive-pressure and negative-pressure pneumatic actuators were directly manufactured using FDM 3D printing [49-51], stereolithography [52], silicone 3D printing [53], and multi-material 3D printing [54-56] to rapidly and easily manufacture soft grippers instead of using conventional silicone molding techniques which require multiple manufacturing steps [57].

In this work, we have developed a 3D printed omni-purpose soft

Manuscript received January --, 2019; This research has been supported by ARC Centre of Excellence for Electromaterials Science (Grant No. CE140100012) and the University of Wollongong, Australia.

Charbel Tawk (ct887@uowmail.edu.au), Andrew Gillett (awg347@uowmail.edu.au), and Gursel Alici (*Corresponding Author, gursel@uow.edu.au.), are with School of Mechanical, Materials, Mechatronic and Biomedical Engineering, and ARC Centre of Excellence for Electromaterials Science, University of Wollongong, AIIM Facility, NSW, 2522, Australia.

Geoffrey M. Spinks (gspinks@uow.edu.au) is with the Intelligent Polymer Research Institute, ARC Centre of Excellence for Electromaterials Science, University of Wollongong, AIIM Facility, NSW, 2522, Australia.

Marc in het Panhuis (panhuis@uow.edu.au) is with the Soft Materials Group, School of Chemistry and Intelligent Polymer Research Institute, ARC Centre of Excellence for Electromaterials Science, University of Wollongong, AIIM Facility, NSW, 2522, Australia.

gripper (OPSOG) capable of grasping a wide variety of objects with different weights, sizes, shapes, textures and stiffnesses. This versatile soft gripper has a unique design where soft 3D printed fingers and a soft 3D printed suction cup operate either simultaneously or separately to pick and place wide variety of objects. Soft linear vacuum actuators (LSOVA) that generate a linear stroke upon activation with vacuum are used to activate the tendon-driven soft fingers. The LSOVA actuators were directly and rapidly manufactured using a low-cost and open-source FDM 3D printer. The actuators have a high blocked force, very fast response, high bandwidth and long lifetime. OPSOG has a payload to weight ratio of 7.06, a maximum gripping force of 31.31N and a tip blocked force of 3.72N. The soft gripper is mounted on a 6-DOF robotic manipulator which is wirelessly controlled through a joystick (i.e. a PlayStation game controller) to pick and place objects in real-time. The user can directly control the position and orientation of the robotic arm and the soft gripper and activate the soft fingers and suction directly through the joystick.

The primary contributions of this study are to: (i) propose a 3D printed omni-purpose soft gripper that is driven by 3D printed soft vacuum actuators, (ii) employ a low cost and single step 3D printing technique using an off-the-shelf soft material to print the support, fingers, suction cup and actuation unit of the gripper, (iii) quantify the performance of the soft actuators and the gripper, and (iv) demonstrate its versatility and dexterity by integrating it on a robotic arm that is controlled wirelessly through a game controller to pick and place a wide variety of objects with different weights, sizes, shapes, textures and stiffnesses.

The remainder of this paper is organized as follows. Section II presents the materials used to fabricate the soft gripper. Section III presents the performance of the LSOVA actuators in terms of step response, blocked force, bandwidth, creep, lifetime and scalability. Section IV presents the finite element and analytical models of LSOVA. Section V presents the principal components of OPSOG. Section VI presents the control architecture of the complete system. Section VII presents the characterization results of OPSOG in terms of grip force, blocked force, payload to weight ratio and grasped objects. Section VIII presents a discussion on the soft gripper as a gold medal winner in the 2018 International Conference on Robotics and Automation (ICRA). Finally, section IX presents the conclusions and future work.

II. Material and Methods

A. OPSOG Materials

The soft gripper was modeled in Autodesk Fusion 360 (Autodesk Inc.). The main components of OPSOG are illustrated in Fig.1. The 3D printed components of OPSOG were 3D printed using an open-source FDM 3D printer (FlashForge Inventor, FlashForge Corporation). The solid support structures of OPSOG were all 3D printed using ABS plastic. The soft actuators, solid and soft supports, soft fingers and soft suction cup were 3D printed and assembled together as shown in Fig. 1. The soft parts of OPSOG were 3D printed using a commercially available thermoplastic poly(urethane) (TPU) known as NinjaFlex (NinjaTek, USA). Distinct colors of the TPU were used to 3D print the soft parts of OPSOG. The soft finger of OPSOG were covered with commercially available soft pads that stick to glass or similar objects with a smooth surface. The pads were cut using a laser cutter (VLS2.30 Desktop, Universal Laser Systems, Inc.) from a commercially available smartphone case (Goo.ey, Gooey Solutions Limited, UK) and were glued to the 3D printed soft fingers. A commercially available thin and flexible fishing lines (46.6kg/dia:0.483mm, GRAND PE WX8, JIGMAN, Japan) were used as tendons to drive the soft fingers. The overall cost of OPSOG which includes the cost of NinjaFlex, ABS, tendons, plastic tubes, soft pads, bolts and nuts is approximately AU$33.

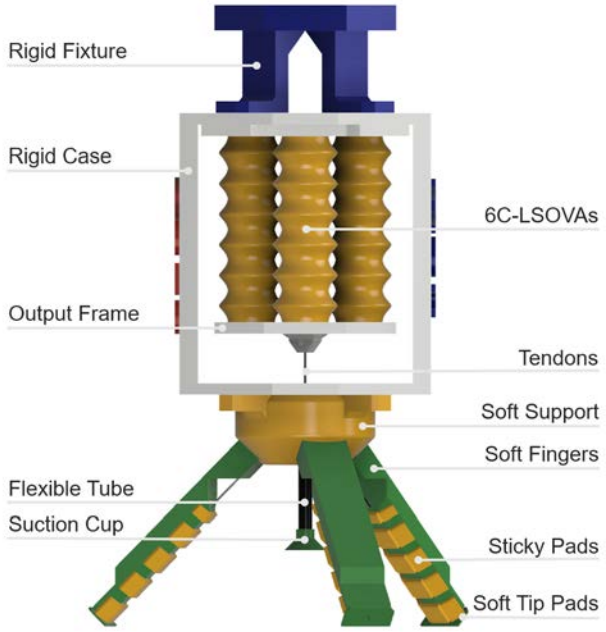

Fig. 1. OPSOG and its main components.

B. TPU Material Model

The stress-strain relationship of the TPU was experimentally obtained for use in the finite element modeling and simulations. Tensile tests were conducted on the TPU according to the ISO 37 standard where the samples were stretched by 800% at a rate of 100mm/s using an electromechanical Instron Universal Testing machine (Instron8801). The average experimental stress-strain data of eight different TPU is shown in Fig. 2. The TPU was modeled as a hyperelastic material. The Mooney-Rivlin 5-parameter model was identified using the average experimental stress-strain curves. The parameters of the hyperelastic material model are listed in Table I. The model was implemented in ANSYS Workbench to perform finite element simulations on the linear soft vacuum actuator to predict its behavior.

TABLE I
TPU HYPERELASTIC MATERIAL MODEL CONSTANTS

Hyperelastic Material Model	Material Constant	Value
Mooney Rivlin	C10	-0.233 MPa
	C01	2.562 MPa
	C20	0.116 MPa
	C11	-0.561 MPa
	C02	0.900 MPa
	Incompressibility Parameter D1	0.000 MPa^{-1}

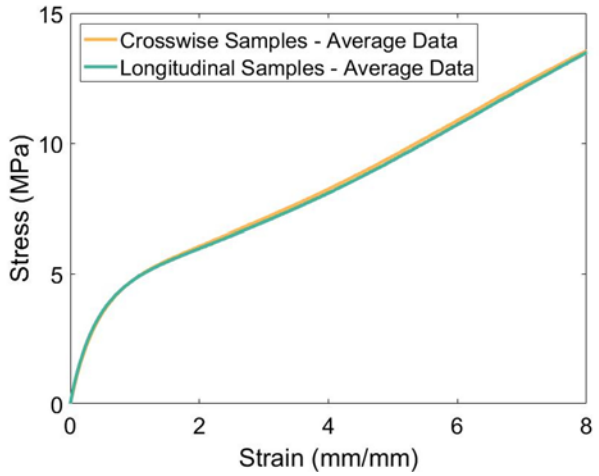

Fig. 2. Average experimental stress-strain curves for crosswise and longitudinal infill patterns

C. Optimized Printing Parameters

The 3D CAD models of LSOVA were sliced using a commercial slicer (Simplify3D LLC, OH, USA). The optimized printing parameters used to print airtight LSOVA are available in our recent publication [51].

III. Vacuum Actuators

The linear soft vacuum actuators used to drive the fingers were fully characterized in a comprehensive study on LSOVAs with up to 5 chambers (5C) prior to their integration in OPSOG. The core of OPSOG was made of four 6C−LSOVA assembled in parallel. Each LSOVA is made of six vacuum chambers (6C) that contract upon activation with 95.7% vacuum to generate a linear stroke. This is the maximum vacuum level that can be generated by the vacuum pump employed. For the sake of completion and clarity, we present the characterization of an improved version of a single 6C−LSOVA actuator in this work. The performance parameters of the 6C-LSOVA and the comparison between the experimental and FEM results are presented in Table II.

TABLE II
6C−LSOVA ACTUATOR PERFORMANCE PARAMETERS

Description, Symbol	Value
Original Length, L_0	81.00 mm
Internal Volume, V_i	23724.82 mm^3
Mass, m	15.02 g
Linear Deformation, δ	39.84 mm
Rise Time, T_r	94 ms
Decay Time, T_d	780 ms
Blocked Force, F_b	30.35 N
Bandwidth, ω_b	2.81 Hz
Lifetime, L_t	26120 Cycles
Experimental Deformation, δ_e	39.84 mm
FEM Deformation, δ_{FEM}	46.85 mm
Difference Between δ_e and δ_{FEM}, $\Delta\delta$	14.10 %
Experimental Blocked Force, $F_{b,exp}$	30.35 N
FEM Blocked Force, $F_{b,FEM}$	30.45 N
Difference Between $F_{b,exp}$ and $F_{b,FEM}$, ΔF_b	0.33 %

A. Step Response

The step response was obtained using a high-resolution laser sensor (Micro-Epsilon, optoNCDT 1700-50) that measures the linear displacement of the actuator upon activation with 95.7% vacuum. The step response of the actuator is shown in Fig. 3 and its rise time and decay time are listed in Table II.

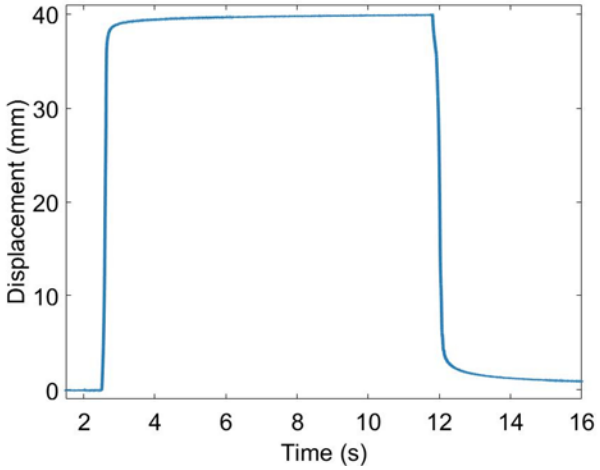

Fig. 3. 6C−LSOVA step response.

B. Blocked Force

The blocked force of the actuator was measured using a force gauge (5000g, FG-5005, Lutron Electronic Enterprise CO., LTD). The actuator was restricted from moving by constraining both ends when 95.7% vacuum was applied to measure the blocked force. The blocked force was 30.35N, as listed in Table II.

C. Bandwidth

The maximum experimental actuation frequency of the 6C−LSOVA was obtained by activating the structure with 95.7% vacuum. The experimental frequency was limited by the speed of the solenoid valves and the inconsistent rate of discharge of the vacuum pump at high frequencies. Consequently, higher actuation frequencies were not achieved due to the limitations imposed by the pneumatic equipment. The bandwidth of the 6C−LSOVA is 2.81Hz as listed in Table II which was estimated from the experimental step response.

D. Creep

The internal pressure of the actuator was kept constant for a period of 35 minutes while its position was monitored to detect any drift resulting from creep. The actuator experienced no creep over this time, as shown in Fig. 4. The pressure of the system did decrease by 1.36% during the experiment but caused negligible change in the actuator stroke. The pressure loss was most likely due to minor air leakage from fittings and connectors.

E. Lifetime

The number of cycles that the actuator sustained before failure is listed in Table II and was measured by activating the actuator using 90% vacuum generated by a DC diagram vacuum pump (Gardner Denver Thomas GmbH). In each actuation cycle, the actuator was activated to achieve full contraction. The internal pressure of LSOVA was returned to atmospheric in each cycle to recover its initial position after it was fully contracted. The actuator performance remained unchanged prior to failure. The 3D printed layers on the corners of the thin walls of the actuator separated which resulted in air gaps in the structure. However, it is important to note that the actuator remained functional after failure and generated a complete stroke under a continuous supply of vacuum which means that LSOVA are fault tolerant.

F. Scalability

We integrated a bundle of four 6C−LOSVA as the primary actuator of OPSOG. The blocked force generated by this bundle of

actuators is 121.40N which is four times the force generated by a single 6C−LSOVA. Therefore, the primary actuator of a gripper typified by OPSOG can be composed of any number of actuators with specific volumes depending on the force required.

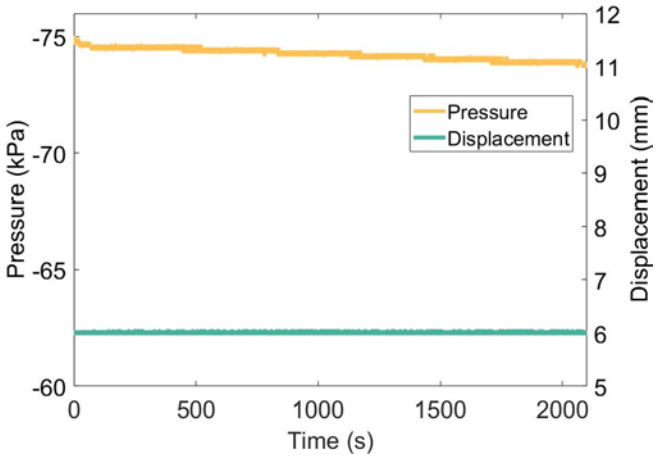

Fig. 4. 6C-LSOVA creep experiment data.

IV. LSOVA FEM AND ANALYTICAL MODELS

A. *LSOVA Finite Element Model*

The CAD model of the 6C–LSOVA was directly imported to ANSYS Design Modeler. The soft actuator was meshed for finite element modeling (FEM) using higher order tetrahedrons. Both ends of the 6C−LSOVA were constrained and a negative pressure was applied on the internal walls. In addition, frictional contact pairs were defined between the internal walls since they touch when the actuators deform. The blocked force and linear deformation of the actuator were predicted using ANSYS Workbench. While the experimental blocked force data matched the FEM results with an acceptable difference as shown in Table II, there is a non-negligible difference between the experimental and FEM strokes. The main reason for this difference is due to the unclean and unsmooth printed upper horizontal walls of the actuators. During the 3D printing process, the first few layers of each horizontal wall sagged and fell due to poor bridging performance by NinjaFlex which resulted in thick plastic residuals that restricted the linear displacement of the LSOVA. This resulted in a smaller stroke than expected from the FEM. The running times of the simulations were 1437s and 130s for the linear deformation and blocked force, respectively. These running times are highly dependent on the amount of memory allocated to ANSYS. This result shows that FEM can be used rapidly and efficiently to predict the behavior of LSOVA. The only challenge encountered was the distortion of elements due to the very high mechanical deformations. However, this issue was alleviated by incorporating a coarser mesh that is suitable for simulating hyperelastic materials undergoing large deformation. The mesh size was studied to ensure that the results are accurate and mesh-independent.

B. *LOSVA Analytical Model*

By employing the free-body diagram of a single chamber of a 6C−LSOVA shown in Fig. 5, we have obtained an analytical model to estimate the blocked force of the actuator. All the parameters of the model are listed in Table III.

TABLE III
6C−LSOVA ANALYTICAL MODEL PARAMETERS

Description, Symbol	Value
Output Force, F_{out}	29.84 N
Pressure Force, F_p	24.71 N
Thin Wall Horizontal Tension, T_x	5.13 N
Input Negative Pressure, P	98.19 kPa
LSOVA Inner Radius, R_i	8.95 mm
LSOVA Outer Radius, R_o	12.99 mm
Radius of Curvature, R_c	0.50 mm
Flattened Frustum Inner Radius, r_i	14.24 mm
Flattened Frustum Outer Radius, r_o	20.67 mm
Flattened Frustum Effective Radius, r_e	17.26 mm
Thin Wall Length, L	6.43 mm
Thin Wall Width, S_e	68.18 mm
LSOVA Angle, θ_c	50.00°
Frustum Effective Angle, θ_e	226.35°

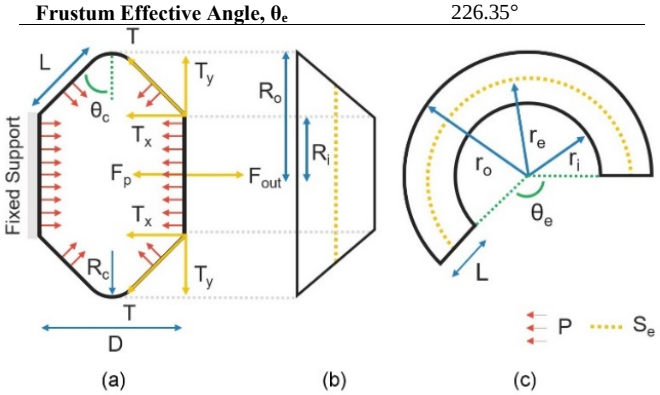

Fig. 5. Free-Body Diagram (FBD). (a) LSOVA FBD (b) Frustum side view (c) Flattened frustum

The output blocked force can be expressed as follows:

$$F_{out} = F_p + 2T_x \tag{1}$$

where

$$F_p = \pi R_i^2 P \tag{3}$$

From Laplace's law, we can write

$$T = R_c P S_e \tag{4}$$

where T is the tension in thin wall and S_e is the effective width of the thin walls which was computed by considering the flattened frustum shown in Fig. 5c. The relationship between LSOVA inner and outer radii and the flattened frustum inner and outer radii can be expressed as follows:

$$r_i = R_i L / (R_o - R_i) \tag{5}$$

$$r_o = R_o L / (R_o - R_i) \tag{6}$$

and the effective radius of the flattened frustum can be computed from the following equation:

$$r_e = L / \ln(r_o / r_i) \tag{7}$$

The effective length of the frustum can be now computed as follows:

$$S_e = r_e \theta_e \tag{8}$$

where

$$\theta_e = (R_o - R_i) / L \tag{9}$$

The horizontal component of the tension can now be written as follows

$$T_x = T \sin\theta_c = R_c P S_e \sin\theta_c \tag{10}$$

Finally, the output blocked force becomes

$$F_{out} = P(\pi R_i^2 + 2R_c S_e \sin\theta_c) \tag{11}$$

Using the data in Table III and comparing with the experimental blocking force in Table II for 6C−LSOVA, the difference between

the experimental and analytical blocked force for 6C−LSOVA is 1.69% and the difference between the analytical and FEM blocked force is 2.0%. This follows that the simple analytical model can be used to predict the blocked force of LSOVA with reasonable accuracy.

V. Design of Principle Components of Opsog

A. LSOVA Actuators

The design of a single vacuum chamber of LSOVA is shown in Fig. 6a. The 6C−LSOVA is made of six identical soft vacuum chambers. The LSOVA actuators generate a linear stroke upon activation with vacuum. The core of the grippers is composed of the actuation unit which is a bundle of four 6C−LSOVA. The four soft actuators were attached to a common rigid output frame that link them directly with the tendons routed through the fingers as shown in Fig.1.

B. Suction Cup

The design of the suction cup is shown in Fig. 6b. The suction cup is printed with thin walls (0.8mm wall thickness) that buckle and conform to objects upon activation. The suction cup is placed in the middle between the three soft fingers which allows both systems to operate either separately or simultaneously without moving.

C. Soft Fingers

Each soft finger is designed with three main faces as shown in Fig. 6c. The multiple faces on each finger allows the gripper to interact with objects from different angles which increases the contact area between the fingers and the grasped objects. This design allows the gripper to grasp objects with irregular shapes and sharp corners. Soft pads that stick to a glossy surface such as glass were placed on the faces of each finger (Fig. 6d). It was observed that these pads increased the friction between the fingers and the grasped objects. Soft 3D printable green pads were added on the tip of the fingers. These pads allow the gripper to grasp flat objects that have a small height compared to their width and length.

VI. Control of Opsog

A. Robotic Manipulator

A 6-DOF robotic manipulator (CRS A465, CRS Robotics Corporation, Canada) was used to move OPSOG in space to pick and place wide variety of objects as shown in Fig. 7 and Video S1. We developed an online method of teleoperation control where the user can control the end-effector position and velocity as well as the soft fingers and suction cup of OPSOG in real-time. We implemented a control system algorithm in LabVIEW (LabVIEW 2017, National Instruments, USA) to support teleoperation and control of the pneumatic equipment of OPSOG.

B. User Input Device

We used a Dual-Shock 4 (DS4) wireless Bluetooth gaming controller (Sony, Australia) that has five analog inputs, 6-axis motion sensor including a 3-axis gyroscope and a 3-axis accelerometer, twelve digital buttons, four digital direction buttons and a two-point capacitive touch pad with a click mechanism. In addition, the DS4 controller contains two eccentric rotating mass vibration motors.

The DS4 was used for differential position control using the five analog inputs and triggers to control the position and orientation of the end-effector. The magnitude of the input on the joysticks correspond to the magnitude of the velocity of the end-effector. Feedback for kinematic errors or controller errors are provided by the controller haptics. The game controller digital buttons are used for fine motion control, opening and closing of the OPSOG fingers, turning on and off the suction cup, saving specific positions and moving to set positions. Using a game controller to wirelessly drive a robot manipulator is a new and effective method for control with the added advantage of being low-cost. Also, it is important to note that the decision of grasping is made solely by the user (i.e. human-in-the-loop control) of this version of the gripper.

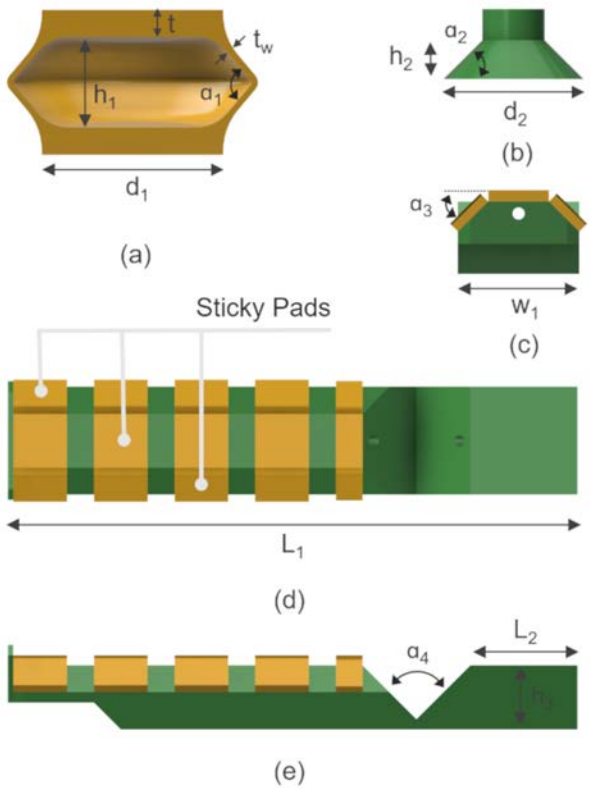

Fig. 6. OPSOG principal components design. (a) LSOVA one unit dimensions: h_1: 10.0, t: 3.0, t_w: 0.80, d_1: 20.0, α_1: 110°, (b) Suction cup dimensions: h_2: 5.0, d_2: 18.0, α_2: 45°. Soft fingers Dimensions (d) Front View: w_1: 20.0, α_3: 45° (d) Top View: L_1: 107.0, (e) Side View: h_3: 12.0, L_2: 20.0, α_4: 45°. All dimensions are in mm.

Fig. 7. CRS 6-DOF robotic manipulator with OPSOG

C. Control Architecture

The control algorithm implemented in LabVIEW was used to control the manipulator by converting the differential position input from the DS4 controller into joint positions (θ1, θ2, θ3, θ4, θ5 and θ6) using analytical inverse kinematic solutions that represent the differential position of the end-effector (Fig. S1. in Video S1). The derived forward and inverse kinematic solutions allow for kinematic constraints to be applied within the implemented algorithm and make it possible to visualize and construct a real-time 3D simulation of the robotic manipulator. The algorithm allows the operator to control the manipulator using one of its inverse kinematic solutions.

VII. Characterization

A. Grip Force

The gripping force (GF) of the actuator was measured using a force sensor (5000g, FG-5005, Lutron Electronic Enterprise CO., LTD). The actuator was activated using 95.7% vacuum when the grasped objects with different shapes were pulled away from the gripper in a vertical direction (Fig. 8). The grip force for the 3D printed cylinder, cube and sphere was measured in three different states where the soft fingers and suction cup (SC) were activated either separately or simultaneously. The grip forces in the three distinct states are listed in Table IV. The maximum grip force was identified before and after disengagement of the suction cup when both the fingers and suction cup were activated. The grip force is highly dependent on the shape, size and texture of the grasped objects. The grip force of the suction cup which depends on its size can be increased by 3D printing suction cups with a larger surface area. However, this suction cup size (Fig. 6b) was used to target objects having small surface area. Also, the grip force of the fingers depends highly on the friction force with the grasped objects. The pads were added to the inner surface of the fingers to enhance the contact friction force between the soft fingers and the grasped objects. Therefore, different suction cups can be used to target specific objects for specific applications. 3D printed suction cups can be replaced and plugged easily and quickly into OPSOG. Finally, the grip force of the fingers can be enhanced by using soft pads that increase the friction force with the grasped objects. The maximum grip force achieved by OPSOG is 31.31N as listed in Table IV. Compared with the grip force of other similar soft grippers reported in the literature, this grip force is comparable with the grip force of silicone molded underactuated grippers [10]. It is higher than the grip force reported in [41,43] and lower than the one reported in [44] for grippers based on fiber-reinforced actuators. It is higher than the grip force reported in [38] and lower than the one reported in [37] for grippers based on PneuNets. It is higher than the grip forces reported in [11,12] for grippers and hands based on hybrid fingers made of soft and rigid materials. It is higher than the blocked force reported in [9] for a gripper based on compliant mechanisms and higher than the blocked forces reported in [49,50] for FDM 3D printed soft actuators. It is reasonable to note that the grip force of OPSOG is lower compared to the grip force of some soft robotic grippers driven by positive pressure actuators. This is due to several reasons such as enhanced gripping capabilities using Gecko-like adhesives in [37] and using positive-pressure soft pneumatic actuators such as PneuNets and fiber-reinforced actuators as the fingers of the soft grippers where the grip force is related to the positive-pressure applied. The grip force increases with an increase in the positive-pressure applied. However, for soft vacuum actuators the output force is limited by the maximum vacuum pressure that can be practically applied.

B. Finger Tip Blocked Force

The blocked force of the soft fingers was measured using a force sensor (5000g, FG-5005, Lutron Electronic Enterprise CO., LTD) when the gripper was activated using 95.7% vacuum. Two fingers were left to move freely upon activation of the soft gripper while the remaining third finger was restricted from moving at its tips where the force sensor was attached normally. The maximum blocked force generated by the soft finger is 3.72N. This blocked force of 3.72N is higher than the tip blocked force reported in [42,43,45,55], lower than the tip force reported in [49] and comparable with the one reported in [9]. The blocked force in [49] is relatively higher compared to the tip force generated by the soft fingers of OPSOG since the fingers of the gripper in [49] are based on positive-pressure bellow-like soft actuators where the grip force is related to the amount of pressure applied.

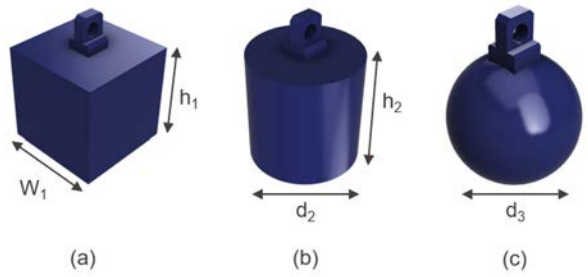

Fig. 8. Grasped Shapes for Grip Force Experiments. (a) Cube: W_1: 28.00, h_1: 28.00 (b) Cylinder: d_2: 28.00, h_2: 28.00 (c) Sphere: d_3: 28.00. All dimensions are in mm.

TABLE IIII.
GRIP FORCE RESULTS

Shape	**Cube**	**Cylinder**	**Sphere**
Description, Symbol	**Value**	**Value**	**Value**
Fingers Only GF, F_F	25.58 N	31.31 N	8.66 N
SC Only GF, F_{SC}	15.79 N	15.61 N	11.31 N
GF Before SC Disengagement, F_{BSC}	18.99 N	21.83 N	12.82 N
GF After SC Disengagement, F_{ASC}	19.33 N	29.02 N	6.59 N

C. Payload of Fingers and Suction Cup

The weight of the gripper including the fixture used to attach it to the robotic arm is 389.69g. We obtained the maximum load lifted by the gripper by activating the soft fingers and suction cup simultaneously. OPSOG lifted a load of 2.7kg when the 6C−LSOVA bundle was activated using 95.7% vacuum. The maximum payload to weight ratio of OPSOG is 7.06. The maximum load of 2.7kg lifted by OPSOG is higher than the load lifted by the soft grippers and hands reported in [9,11,41-43,45,50] and lower than the load lifted by the soft grippers activated by positive pressure in [13,37,44,49]. The load lifted by other similar soft grippers that OPSOG outperformed in terms of grip force and blocked force was not reported [10,12,38,55].

D. Grasped Objects

The gripper can pick and place a wide variety of objects with different weights, shapes, stiffnesses and textures as shown in Fig. S2 in Video S1 and Video S1. The objects grasped in Video S1 were chosen based on the common objects used in daily activities. The soft fingers and suction cup of OPSOG were activated either separately or simultaneously where the gripping was achieved using both systems. For the gripping process, the suction cup was activated

first if there was enough room for it to attach to the grasped object. Then, the fingers were activated to achieve a firm and stable grip. In this case, the fingers acted as a support for the grasped objects. The soft fingers wrapped around the grasped object after activating the suction cup to provide an additional support and a firm grip during the movement of the robotic manipulator. This approach is crucial since it enhances the range of objects the gripper can grasp and interact with and it provides a firm grip during movement and against external disturbances as shown in Video S1. OPSOG showed its versatility and dexterity and the effectiveness of using suction cups along with soft fingers to grasp and manipulate wide variety of objects. However, it is important to note that OPSOG is not capable of picking and placing very large objects compared to its size.

VIII. Discussion

A. OPSGO Gripper

The OPSOG gripper can grasp a wide variety of objects with different weights, sizes, shapes, textures and stiffnesses. In addition, OPSOG can be used in wide variety of picking and placing applications where rigid and soft objects are involved. The gripper is lightweight and has a low manufacturing cost. OPSOG is 3D printed from commercially available low-cost materials using a low-cost and open-source FDM 3D printer. This feature drastically reduces the replacement and maintenance costs and makes it suitable for do-it-yourself (DIY) applications. Moreover, OPSOG is customizable. The gripper can be designed to meet specific or desired requirements for specific applications. First, the core of OPSOG, which is the set of linear actuators, can be scaled depending on the force required or desired for a specific application. Second, the stiffness and the softness of the soft fingers can be changed by changing some printing parameters such as infill percentage and the number of flexural joints in each finger. Third, the suction cup can be easily replaced and sized according to specific applications.

B. ICRA 2018 Soft Material Robot Challenge

This competition aimed to determine the most effective soft robot for gripping tasks. Objects with various weights, sizes, shapes and stiffnesses were set for the soft gripper to grip and transport. The objects included a baseball cap, a banana, an apple, a pair of scissors, a tissue box, a power bank, a USB memory stick, a shuttlecock, a notebook, a chewing gum box, a cotton swab box, a potato chips bag, a double-faced adhesive tape, a bar of soap and a bunch of grapes. OPSOG installed at the end point of a robot manipulator (Video S1) picked and placed all the specified objects successfully. OPSOG showed its versatility and effectiveness in soft robotic applications by picking and placing the different objects successfully.

IX. Conclusions and Future Work

In this work, we have developed and evaluated the performance of a 3D printed soft gripper using a low-cost and open source FDM 3D printer. The grasping is achieved using soft 3D printable tendon-driven fingers and a suction cup that operate either separately or simultaneously. The tendon-driven soft fingers were actuated using a bundle of directly 3D printed soft actuators that generate a linear stroke upon activation with vacuum. The soft actuators were fully characterized, and their performance was predicted using finite element and an analytical model. The OPSOG gripper can grasp a wide variety of objects with different weights, sizes, shapes, textures and stiffnesses. The gripper was integrated on a 6-DOF robotic manipulator that was controlled wirelessly using a gaming controller. A control algorithm was implemented to allow a user to move the robotic manipulator in space and to control the pneumatic equipment including the vacuum pump and solenoid valves. In this work, the robot arm was controlled solely by the user and no feedback control was implemented. In future work, a high-definition camera will be added to OPSOG to analyze the objects being grasped. A machine learning algorithm will be implemented to identify different objects in space and pick them depending on their position, size and shape. The algorithm will dictate the most suitable orientation for picking and handling the objects as well using the soft fingers and suction cup either separately or simultaneously. Also, a model will be developed for the soft fingers to identify how the force is transmitted from the LSOVA to the soft fingers. In this work, modeling the soft actuators was the first step toward developing a full model for the entire gripper.

References

[1] S. I. Rich, R. J. Wood, and C. Majidi, “Untethered soft robotics,” *Nat. Electron.*, vol. 1, no. 2, pp. 102-112, 2018.

[2] B. Trimmer, “Soft robots,” *Curr. Biol*, vol. 23, no. 15, pp. R639-R641, 2013.

[3] D. Rus, and M. T. Tolley, “Design, fabrication and control of soft robots,” *Nature*, vol. 521, pp. 467, 2015.

[4] D. Trivedi, C. D. Rahn, W. M. Kier, and I. D. Walker, “Soft Robotics: Biological Inspiration, State of the Art, and Future Research,” *Appl. Bionics Biomech.*, vol. 5, no. 3, 2008.

[5] L. Biagiotti, F. Lotti, C. Melchiorri and G. Vassura, “How Far is the Human Hand: A Review on Anthropomorphic Robotic End-effectors,” University of Bologna, Bologna, Italy, 2004.

[6] K. Tai, A.-R. El-Sayed, M. Shahriari, M. Biglarbegian, and S. Mahmud, “State of the Art Robotic Grippers and Applications,” *Robotics*, vol. 5, no. 2, pp. 11, 2016.

[7] S. Jun, C. Vito, F. Dario, and S. Herbert, “Soft Robotic Grippers,” *Adv. Mater*, vol. 30, no. 29, pp. 1707035, 2018.

[8] R. Mutlu, G. Alici, M. in het Panhuis and G. Spinks, "3D Printed Flexure Hinges for Soft Monolithic Prosthetic Fingers", *Soft Robot.*, vol. 3, no. 3, pp. 120-133, 2016.

[9] F. Chen et al., "Topology Optimized Design, Fabrication, and Characterization of a Soft Cable-Driven Gripper," *IEEE Robot. Autom. Lett.*, vol. 3, no. 3, pp. 2463-2470, 2018.

[10] M. Manti, T. Hassan, G. Passetti, N. D'Elia, C. Laschi, and M. Cianchetti, “A Bioinspired Soft Robotic Gripper for Adaptable and Effective Grasping,” *Soft Robot.*, vol. 2, no. 3, pp. 107-116, 2015.

[11] A. K. Mishra, E. Del Dottore, A. Sadeghi, A. Mondini, and B. Mazzolai, “SIMBA: Tendon-Driven Modular Continuum Arm with Soft Reconfigurable Gripper,” *Front. Robot. AI*, vol. 4, no. 4, 2017.

[12] R. R. Ma, L. U. Odhner, and A. M. Dollar, "A modular, open-source 3D printed underactuated hand," in *Proc. IEEE Int. Conf. Robot. Autom.*, 2013, pp. 2737-2743.

[13] L. U. Odhner et al., "A compliant, underactuated hand for robust manipulation," *Int. J Robot. Res.*, vol. 33, no. 5, pp. 736-752, 2014.

[14] MultiChoiceGripper | Festo Corporate, Festo.com, 2013.

[15] W. Crooks, G. Vukasin, M. O’Sullivan, W. Messner, and C. Rogers, “Fin Ray® Effect Inspired Soft Robotic Gripper: From the RoboSoft Grand Challenge toward Optimization,” *Front. Robot. AI*, vol. 3, no. 70, 2016.

[16] J. Hu, D. Erbao, X. Min, L. Chunshan, G. Alici, and J. Yang, “Soft and smart modular structures actuated by shape memory alloy (SMA) wires as tentacles of soft robots,” *Smart Mater. Struct*, vol. 25, no. 8, pp. 085026, 2016.

[17] Y. She, C. Li, J. Cleary, and H.-J. Su, “Design and Fabrication of a Soft Robotic Hand With Embedded Actuators and Sensors,” *J. of Mechanisms and Robotics*, vol. 7, no. 2, pp. 021007-021007-9, 2015.

[18] W. Wei, and A. Sung-Hoon, “Shape Memory Alloy-Based Soft Gripper with Variable Stiffness for Compliant and Effective Grasping,” *Soft Robot.*, vol. 4, no. 4, pp. 379-389, 2017.

[19] H.-I. Kim, M.-W. Han, S.-H. Song, and S.-H. Ahn, “Soft morphing hand driven by SMA tendon wire,” *Compos. Part B Eng.*, vol. 105, pp. 138-148, 2016.

[20] R. Hugo, W. Wang, B. Binayak, and A. Sung-Hoon, “Fabrication of wrist-like SMA-based actuator by double smart soft composite casting,” *Smart Mater. Struct*, vol. 24, no. 12, pp. 125003, 2015.

[21] Q. Ge, A. H. Sakhaei, H. Lee, C. K. Dunn, N. X. Fang, and M. L. Dunn, “Multimaterial 4D Printing with Tailorable Shape Memory Polymers,” *Sci. Rep*, vol. 6, pp. 31110, 2016.

[22] B. Marc, K. Karl, Z. Jörg, N. Ulrich, and L. Andreas, “Reversible Bidirectional Shape-Memory Polymers,” *Adv. Mater*, vol. 25, no. 32, pp. 4466-4469, 2013.

[23] W. Wang, C. Li, M. Cho, and S.-H. Ahn, “Soft Tendril-Inspired Grippers: Shape Morphing of Programmable Polymer–Paper Bilayer Composites,” *ACS Appl. Mater. Interfaces*, vol. 10, no. 12, pp. 10419-10427, 2018.

[24] O. A. Araromi, I. Gavrilovich, J. Shintake, S. Rosset, M. Richard, V. Gass, and H. R. Shea, “Rollable Multisegment Dielectric Elastomer Minimum Energy Structures for a Deployable Microsatellite Gripper,” *IEEE/ASME Trans. Mechatronics*, vol. 20, no. 1, pp. 438-446, 2015.

[25] S. Jun, R. Samuel, S. Bryan, F. Dario, and S. Herbert, “Versatile Soft Grippers with Intrinsic Electroadhesion Based on Multifunctional Polymer Actuators,” *Adv. Mater*, vol. 28, no. 2, pp. 231-238, 2016.

[26] J. Guo, K. Elgeneidy, C. Xiang, N. Lohse, L. Justham, and J. Rossiter, “Soft pneumatic grippers embedded with stretchable electroadhesion,” *Smart Mater. Struct*, vol. 27, no. 5, pp. 055006, 2018.

[27] H. Yuk, S. Lin, C. Ma, M. Takaffoli, N. X. Fang, and X. Zhao, “Hydraulic hydrogel actuators and robots optically and sonically camouflaged in water,” *Nat. Commun*, vol. 8, pp. 14230, 2017.

[28] E. Palleau, D. Morales, M. D. Dickey, and O. D. Velev, “Reversible patterning and actuation of hydrogels by electrically assisted ionoprinting,” *Nat. Commun*, vol. 4, pp. 2257, 2013.

[29] D. Han, C. Farino, C. Yang, T. Scott, D. Browe, W. Choi, J. W. Freeman, and H. Lee, “Soft Robotic Manipulation and Locomotion with a 3D Printed Electroactive Hydrogel,” *ACS Appl. Mater. Interfaces*, vol. 10, no. 21, pp. 17512-17518, 2018.

[30] W. J. Zheng, N. An, J. H. Yang, J. Zhou, and Y. M. Chen, “Tough Al-alginate/Poly(N-isopropylacrylamide) Hydrogel with Tunable LCST for Soft Robotics,” *ACS Appl. Mater. Interfaces*, vol. 7, no. 3, pp. 1758-1764, 2015.

[31] R. C. Richardson, M. C. Levesley, M. D. Brown, J. A. Hawkes, K. Watterson, and P. G. Walker, “Control of ionic polymer metal composites,” *IEEE/ASME Trans. Mechatronics*, vol. 8, no. 2, pp. 245-253, 2003.

[32] R. Lumia, and M. Shahinpoor, “IPMC microgripper research and development,” *J.Phys. Conf. Ser*, vol. 127, no. 1, pp. 012002, 2008.

[33] O. Manuel, C. Girish, and Z. Babak, “Laser-micromachined cellulose acetate adhesive tape as a low-cost smart material,” *J. Polym. Sci. B*, vol. 51, no. 17, pp. 1263-1267, 2013.

[34] T. Silvia, G. Francesco, S. Edoardo, M. Alessio, M. Barbara, and M. Virgilio, “Toward a New Generation of Electrically Controllable Hygromorphic Soft Actuators,” *Adv. Mater*, vol. 27, no. 10, pp. 1668-1675, 2015.

[35] T. Wang, L. Ge, and G. Gu, “Programmable design of soft pneu-net actuators with oblique chambers can generate coupled bending and twisting motions,” *Sens. Actuators, A*, vol. 271, pp. 131-138, 2018.

[36] G. Alici, T. Canty, R. Mutlu, W. Hu and V. Sencadas, "Modeling and Experimental Evaluation of Bending Behavior of Soft Pneumatic Actuators Made of Discrete Actuation Chambers", *Soft Robot.*, vol. 5, no. 1, pp. 24-35, 2018.

[37] P. Glick, S. A. Suresh, D. Ruffatto, M. Cutkosky, M. T. Tolley, and A. Parness, “A Soft Robotic Gripper With Gecko-Inspired Adhesive,” *IEEE Robot. Autom. Lett.*, vol. 3, no. 2, pp. 903-910, 2018.

[38] Y. Hao, Z. Gong, Z. Xie, S. Guan, X. Yang, Z. Ren, T. Wang, and L. Wen, "Universal soft pneumatic robotic gripper with variable effective length." in *Proc. 2016 35th Chinese Control Conf.*, 2016, pp. 6109-6114. pp. 6109-6114.

[39] S. Terryn, J. Brancart, D. Lefeber, G. Van Assche, and B. Vanderborght, “Self-healing soft pneumatic robots,” *Sci. Robot.*, vol. 2, no. 9, 2017.

[40] Core Technology, Soft Robotics, softroboticsinc.com, 2018.

[41] R. Deimel, and O. Brock, “A novel type of compliant and underactuated robotic hand for dexterous grasping,” *Int. J. Robot. Res.*, vol. 35, no. 1-3, pp. 161-185, 2016.

[42] R. Deimel and O. Brock, "A compliant hand based on a novel pneumatic actuator," in *Proc. 2013 IEEE Int. Conf. Robot. Autom.*, 2013, pp. 2047-2053.

[43] J. Fraś, M. Maciaś, F. Czubaczyński, P. Sałek, and J. Główka, "Soft Flexible Gripper Design, Characterization and Application," in *Proc. of the International Conference SCIT*, 2016, pp. 368-377.

[44] J. Zhou, S. Chen, and Z. Wang, "A Soft-Robotic Gripper With Enhanced Object Adaptation and Grasping Reliability," *IEEE Robot. Autom. Lett.*, vol. 2, no. 4, pp. 2287-2293, 2017

[45] H. Zhang, A. S. Kumar, J. Y. H. Fuh, and M. Y. Wang, "Topology optimized design, fabrication and evaluation of a multimaterial soft gripper," in *Proc. IEEE Int. Conf. Soft Robot.*, 2018, pp. 424-430.

[46] E. Brown, N. Rodenberg, J. Amend, A. Mozeika, E. Steltz, M. R. Zakin, H. Lipson, and H. M. Jaeger, “Universal robotic gripper based on the jamming of granular material,” *Proc. Natl. Acad. Sci.*, vol. 107, no. 44, pp. 18809-18814, 2010.

[47] OctopusGripper | Festo Corporate, Festo.com, 2017.

[48] S. Li, D. M. Vogt, D. Rus, and R. J. Wood, “Fluid-driven origami-inspired artificial muscles,” *Proc. Natl. Acad. Sci.*, vol. 114, no. 50, pp. 13132-13137, 2017.

[49] H. K. Yap, H. Y. Ng, and C.-H. Yeow, “High-Force Soft Printable Pneumatics for Soft Robotic Applications,” *Soft Robot.*, vol. 3, no. 3, pp. 144-158, 2016.

[50] B. A. W. Keong and R. Y. C. Hua, "A Novel Fold-Based Design Approach toward Printable Soft Robotics Using Flexible 3D Printing Materials," *Adv. Mater. Technol.*, vol. 3, no. 2, p. 1700172, 2018.

[51] C. Tawk, M. in het Panhuis, G.M, Spinks, and G. Alici, "Bioinspired 3D Printable Soft Vacuum Actuators (SOVA) for Locomotion Robots, Grippers and Artificial Muscles", *Soft Robot.*, vol. 5, no. 6, pp. 685-694, 2018.

[52] N. P. Bryan, J. W. Thomas, Z. Huichan, and F. S. Robert, "3D printing antagonistic systems of artificial muscle using projection stereolithography," *Bioinspir. Biomim.*, vol. 10, no. 5, p. 055003, 2015.

[53] O. D. Yirmibesoglu *et al.*, "Direct 3D printing of silicone elastomer soft robots and their performance comparison with molded counterparts," in *Proc. IEEE Int. Conf. Soft Robot.*, 2018, pp. 295-302.

[54] R. MacCurdy, R. Katzschmann, K. Youbin, and D. Rus, "Printable hydraulics: A method for fabricating robots by 3D co-printing solids and liquids," in *Proc. IEEE Int. Conf. Robot. Autom.*, 2016, pp. 3878-3885.

[55] Z. Wang, and S. Hirai, “Soft Gripper Dynamics Using a Line-Segment Model With an Optimization-Based Parameter Identification Method,” *IEEE Robot. Autom. Lett.*, vol. 2, no. 2, pp. 624-631, 2017.

[56] D. Drotman, S. Jadhav, M. Karimi, P. deZonia, and M. T. Tolley, "3D printed soft actuators for a legged robot capable of navigating unstructured terrain," in *Proc. IEEE Int. Conf. Robot. Autom., 2017*, pp. 5532-5538.

[57] A. D. Marchese, R. K. Katzschmann, and D. Rus, "A Recipe for Soft Fluidic Elastomer Robots," *Soft robot.*, vol. 2, no. 1, pp. 7-25, 2015.